HIGH-FREQUENCY CALIBRATION OF WALL-PRESSURE SENSORS

E. Salze, C. Desjouy, E. Jondeau & S. Ollivier

Laboratoire de Mécanique des Fluides et d'Acoustique
UMR CNRS 5509, École Centrale de Lyon, Université de Lyon
36, avenue Guy de Collonge, 69131 ECULLY Cedex, France
edouard.salze@ec-lyon.fr

INTRODUCTION

In this communication, high-frequency calibration of wall-pressure sensors is performed.

The first motivation is the investigation of wall-pressure fluctuations for automotive or air transportation applications [1]. Wall-pressure fluctuations are associated with the indirect contribution to cabin noise through panel vibrations. In this context, wall-pressure spectra are investigated using an array of remote flush-mounted sensors [2,3]. A reliable and high-frequency calibration procedure is needed to take into account the mounting of the sensors.

In the context of high-speed compressors studies, a second motivation of the present work is to perform reliable descriptions of instabilities sources at high rotation speeds. This requires high-frequency sensors (typically up to tens of kHz) with a large dynamic range (thousands of Pa). For this purpose, flush-mounted piezoresistive sensors may be used [4]. Shock-tube facilities can be used to obtain the resonance frequency and an estimation of the frequency response of such sensors [5]. However, the pressure step obtained inside a shock-tube facility cannot be precisely determined and reproduced [6].

In this work, two calibration methods are considered in order to cover a wide frequency range. First, a low-frequency calibration (100Hz-12kHz) is performed using a loud-speaker mounted into a vinyl tube, and a reference transducer. This method is valid up to the cut-off frequency of the reference transducer, typically up to 12 kHz. Second, a high-frequency calibration method is applied. This method involves an electrical spark discharge as an acoustic source. The pressure wave emitted by the spark source is determined using a reference sensor, for example an 1/8 in. microphone. The frequency response of the pressure sensor is then obtained by comparison between the pressure wave and the output signal of the pressure sensor. This method is valid up to the frequency cutoff of the reference sensor. The frequency range of this method can be improved if the pressure wave is deduced from optical measurements [7]. This approach has been recently developed in the framework of project SIMMIC, funded by the French National Research Agency [8,9].

In the present study, the high-calibration method is applied. The objective of this work is to combine the high-frequency calibration to a low frequency calibration in order to extend the frequency range. Two kinds of wall-pressure sensors, used for aeronautical or turbomachinery applications, have been calibrated to illustrate this principle. The first is a wall-mounted microphone inside a pinhole cap. The second is a wall-mounted MEMS pressure sensor.

I. EXPERIMENTAL METHOD

a- Low-frequency calibration

The low-frequency calibration (100Hz-12kHz) is achieved by using a loud-speaker. The calibration is performed by comparison between the probe to be calibrated and a flush-mounted sensor. A white noise is emitted in the frequency range from 100 Hz to 20 kHz, which propagates through a calibration tube (see Fig. 1). A reference microphone is mounted near the open end of the tube. The sensor is calibrated following a two-step procedure.

In the first step, the calibration tube is positionned above the sensor to be calibrated. The complex transfer function F_1 between the reference sensor and the sensor to be calibrated is measured. The transfer function F_1 depends upon the frequency responses of the probe to be calibrated

and the reference sensor, respectively noted H and H_{ref}, as:

$$F_1 = \frac{H}{H_{\text{ref}}} \tag{1}$$

In the second step, the calibration tube is positionned above a flush-mounted sensor (1/8 in. Brüel & Kjaer microphone without its protection grid), and the complex transfer function F_2 between the reference sensor and the flush-mounted sensor is measured. The transfer function F_2 depends upon the frequency response of the flush-mounted sensor as:

$$F_2 = \frac{H_{\text{flush}}}{H_{\text{ref}}} \tag{2}$$

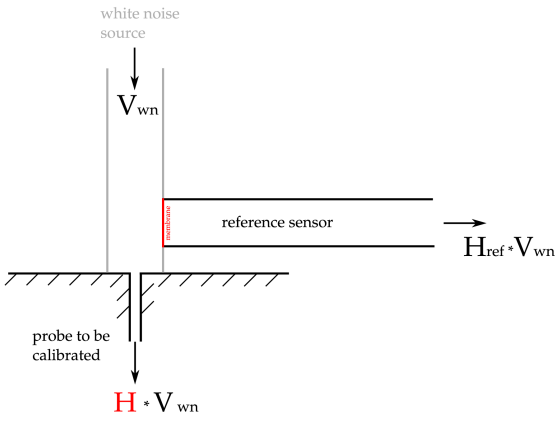

Fig. 1: Low-frequency calibration of a wall-pressure sensor, using a loud-speaker and a reference sensor.

Assuming that, over the considered frequency range (100 Hz – 12 kHz), the frequency response of the flush-mounted sensor is flat, *ie* $H_{\text{flush}} = 1$, the complex frequency response H of the probe to be calibrated is obtained as:

$$H = \frac{F_1}{F_2} \tag{3}$$

This method is valid up to the frequency cut-off of the flush-mounted sensor or the reference sensor, or the frequency cut-off of the calibration tube, whichever frequency cut-off is the smallest. In the present experiment, the calibration tube has the smallest cut-off frequency, around 12 kHz.

b- High-frequency calibration

To overcome the frequency limitations of the method presented in paragraph I.a, a high-frequency calibration is achieved by using an electrical spark source emitting short duration and high pressure spherical waves [10].

The electrical spark source is made of two tungsten electrodes, separated by a gap of 20 mm, connected to a high voltage electrical supply. The voltage is set to obtain a spark every second approximately. The sudden local heating generates a high amplitude and short duration pressure pulse. Because of nonlinear propagation, a shockwave is formed a few centimeters away from the electrodes (see Fig. 2).

At a distance of 30 cm away from the electrodes, the peak pressure is about 800 Pa and rapidly decreases with the distance [11]. Thanks to the high repetition rate of the source, the experiment can be performed several times (typically with 100 spark shots) in order to average the resulting frequency response. Reflections are also easily eliminated by windowing the signals in the time domain.

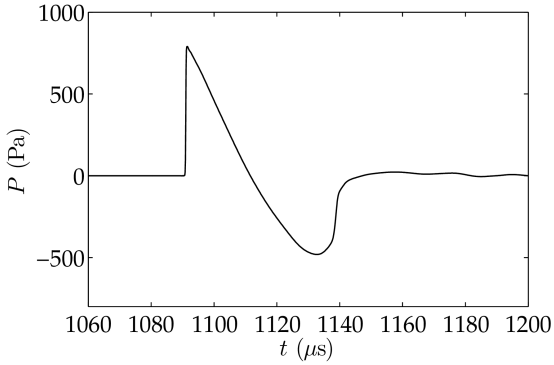

Fig. 2: Pressure wave emitted by the electrical spark source, measured at a distance r = 30 cm from the electrodes.

The high-frequency calibration is performed by comparison to a reference sensor (see Fig. 3). The sensor to be calibrated and the reference sensor are flush-mounted on a plane baffle in order to reduce diffraction effects on the edge of the sensor. The baffle is positionned at a distance r = 20 cm from the spark source.

The output voltages of the reference sensor and of the sensor to be calibrated are simultaneously measured over a sampling frequency of 10 MHz using a National Instrument NI-5105 acquisition card. The output voltage of the sensor to be calibrated and the reconstructed pressure wave are then compared, and the complex transfer function of the sensor is deduced. This approach is valid up to the cutoff frequency of the reference sensor, which is around 140 kHz for a Brüel & Kjær type 4138 1/8 in. microphone [9].

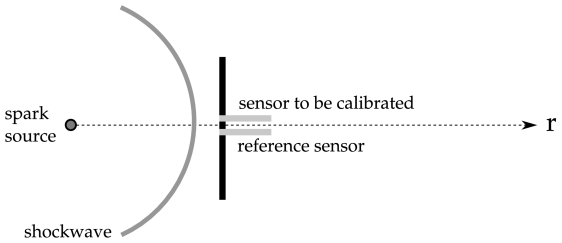

Fig. 3: High-frequency calibration of a wall-pressure sensor, using a spark source and a reference sensor.

A much wider frequency range of hundreds of kHz can be achieved by using optical measurements instead of a conventionnal reference sensor. The principle of a Mach-Zender interferometer used as a high-frequency pressure sensor has been proposed by Smeets [12]. The reconstruction procedure to obtain the pressure wave has been developed later by Yuldashev [7].

A laser beam is splitted in two (see Fig. 4). The two identical laser beams are then reflected on mirror, and combined through another beam splitter. The resulting light beam then hits a photodiode sensor. When the pressure wave travels across the first light beam, a phase difference appears between the two light beams. The pressure wave is reconstructed from the phase difference between the two laser beams. A detailed description of the reconstruction procedure can be found in [7].

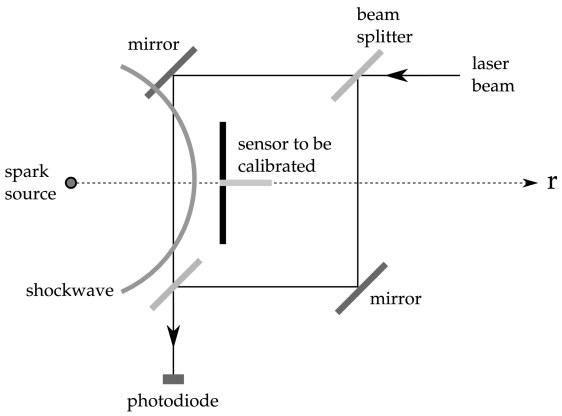

Fig. 4: High-frequency calibration of a wall-pressure sensor, using a spark source and a Mach-Zender interferometer [7].

c- Wall-pressure sensors mountings

In the following, two kinds of wall-pressure sensors are considered and calibrated.

The first is a Brüel & Kjær type 4138 1/8 in. condenser microphone, mounted without its protection grid. The sensing area of the microphone has been reduced by fitting it with a pinhole cap (see Fig. 5). This mounting allows the reduction of spatial averaging for turbulent boundary-layers characterisations [3]. The microphone is connected to a Brüel & Kjær type 2670 preamplifier. A Brüel & Kjær Nexus amplifier, whose frequency response has been extended (-3 dB cutoff at 200 kHz), is used. This sensor has been calibrated in the high-frequency domain using another Brüel & Kjær 1/8 in. condenser microphone as a reference sensor.

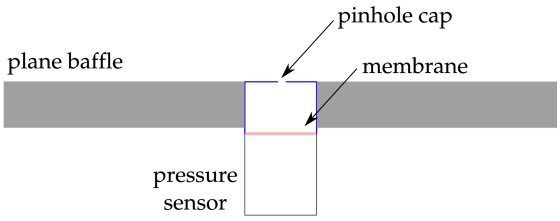

Fig. 5: Mounting of the Brüel & Kjær type 4138 1/8 in. microphone inside a pinhole cap.

The second pressure sensor considered in this study is a 0.152 in. diameter flush-mounted Kulite 190-M 1PSI wall-pressure sensor. The wall-pressure sensor is mounted with its protection grid into a plane baffle (see Fig. 6). A continous 12 V battery power supply is used. This sensor has been calibrated in the high-frequency domain using the Mach-Zender interferometer as a reference sensor.

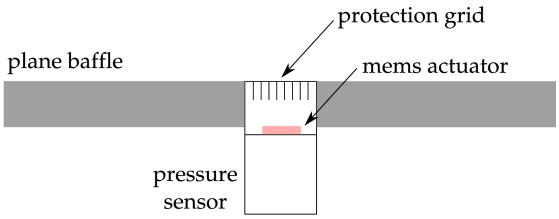

Fig. 6: Mounting of the Kulite 190-M pressure sensor.

II. RESULTS AND DISCUSSION

a- Condenser microphone behind a pinhole

The low-frequency response of the 1/8 in. microphone behind the pinhole cap has been measured using the method described in Sec. I.a. The low-frequency response is plotted in Fig. 7 as a gray line up to 12 kHz, which is the cutoff frequency of the calibration tube. The high-frequency response has been obtained using a flush-mounted 1/8 in. microphone as a reference sensor (see Fig. 3). The response is plotted as a black dashed line up to 50 kHz (see Fig. 7). Below 4 kHz, the shockwave contains very few energy. In

the low-frequency domain below 5 kHz, the response of the sensor is flat. A sensitivity of 0.47 mV/Pa is obtained at a frequency of 1 kHz. The peak around 20 kHz is associated with the resonance of the pinhole cavity (see Fig. 5).

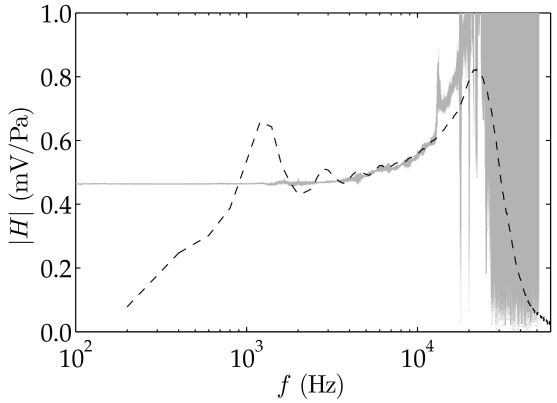

Fig. 7: Frequency response of the 1/8 in. microphone behind the pinhole cap. Gray line: low-frequency (100 Hz – 12 kHz) calibration using a loud-speaker. Black dashed line: high-frequency (4 kHz – 50 kHz) calibration using a spark source.

In the frequency range from 4 kHz to 12 kHz, an excellent agreement, within less than 5% difference for the response amplitude, is obtained between the two methods (low and high frequency). The two responses have therefore been combined in order to provide a frequency response in the range from 100 Hz to 50 kHz. The resulting frequency response has been used to correct wall-pressure measurements [3].

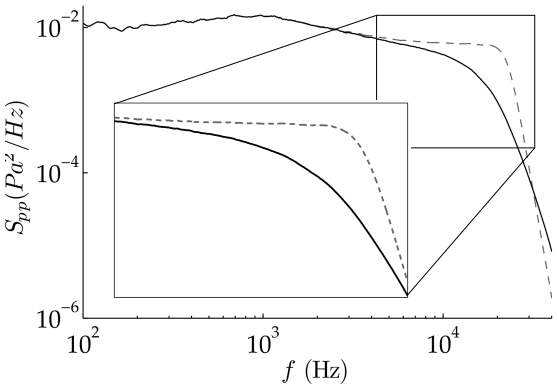

Fig. 8: Measured wall-pressure spectrum beneath a turbulent boundary-layer, in a wind tunnel, at a flow speed of 45 m/s [3]. Gray dashed line: rough spectrum. Solid black line: corrected spectrum using the frequency response from Fig. 7. Bottom-left corner: close view between 5 kHz and 30 kHz.

The wall-pressure spectrum, measured inside a wind tunnel at a flow velocity of 45 m/s, is plotted in Fig. 8. The rough spectrum is plotted using a dashed gray line. The resonance of the pinhole cap is visible around 20 kHz. The corrected spectrum is found in very good agreement with previously published experimental and numerical data and with semi-empirical models from the literature [3], which validates our approach.

b- Flush-mounted MEMS sensor

The low-frequency calibration of the flush-mounted Kulite 190M sensor has been performed using the method described in Sec. I.a. The low-frequency response is plotted in Fig. 10 as a black line. In the low-frequency domain below 6 kHz, the reponse of the sensor is flat within about 5 %. A sensitivity of 11.67 µV/Pa is obtained at a frequency f = 1 kHz. Considering the doubling in sensitivity resulting from the pressure doubling at the wall, a good agreement with the value of the manufacturer is obtained, within about 10%.

The high-frequency calibration has been performed using the Mach-Zender interferometer as a reference sensor. The output voltage of the Kulite sensor, submitted to the spark source, is plotted in Fig. 9. Compared to the input pressure wave (see Fig. 2), the output voltage exhibits different features. The pressure rise time is of the order of 0.3 µs [7], whereas the output voltage rise time is of the order of 5 µs. The output voltage of the sensor contains oscillations, at a time period of about 13 µs. These oscillations remain long after the pressure is not applied. The resonance of the transducer appears to be weakly damped.

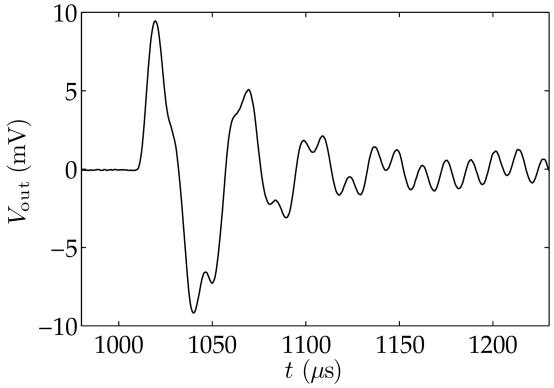

Fig. 9: Output voltage of the Kulite 190-M pressure sensor, submitted to the pressure wave (see Fig. 2).

The output voltage from Fig. 9 and the pressure wave have been compared to obtain the frequency response of the wall-pressure sensor (see Fig. 10). In the frequency range from 4 kHz to 12 kHz, the two calibration curves collapse within about 50 %, which allows the combination of the two methods.

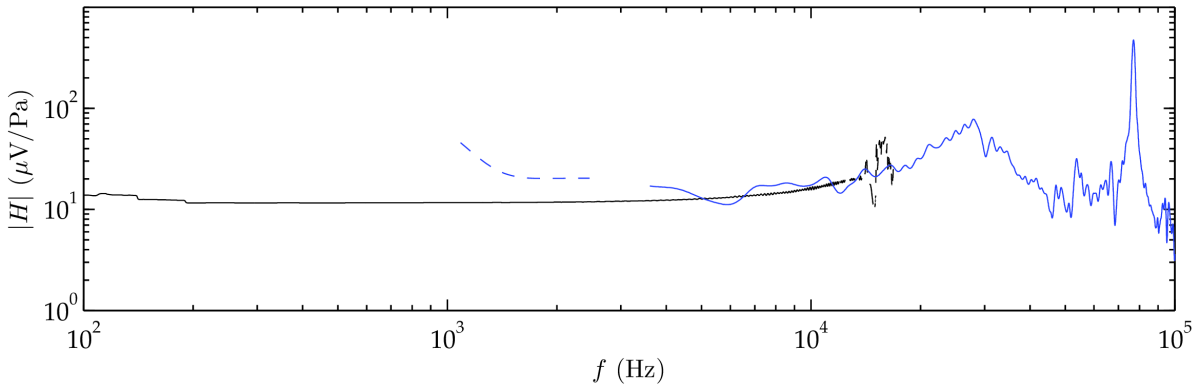

Fig. 10: Frequency response of the 190-M Kulite pressure transducer. Black line: low-frequency calibration using a loud-speaker. Blue line: high-frequency calibration using a spark source and a Mach-Zender interferometer. Dashed lines: frequency ranges of low energy (above 12 kHz for the loud-speaker and below 3 kHz for the spark source).

Two peaks can be identified on the sensor frequency response. The first peak appears at a frequency f = 30 kHz, and the second at a frequency f = 77 kHz. A frequency of 77 kHz corresponds to a period of about 13 µs, which was seen on the output voltage of the pressure sensor (see Fig. 9). The narrow peak around 77 kHz is therefore likely to be the resonance of the MEMS actuator. The first peak around 30 kHz is currently examined. For turbomachinery applications, the resulting frequency responses may be applied as corrections to wall-pressure measurements below the resonance frequency of the sensor.

CONCLUSION

In the present work, two calibration methods have been successfully applied and combined to characterise wall-pressure sensors in a wide frequency range. The first method is performed using a loud-speaker. It covers the frequency range from 100 Hz to 12 kHz. The second method involves a spark discharge as an acoustic source, and a reference sensor. It is valid in the frequency range from a few kHz to the cutoff frequency of the reference sensor.

Those two methods have been applied to a Brüel & Kjaer type 4138 1/8 in. microphone, flush-mounted behind a pinhole cap, with an excellent agreement. The resulting frequency response has been successfully used to correct wall-pressure measurements beneath a turbulent boundary-layer [3]. A Kulite 190-M wall-pressure sensor has also been investigated. A good agreement is found between the two methods in the frequency range from 4 kHz to 12 kHz. In the low-frequency domain below 4 kHz, the response of the transducer is flat. The low-frequency sensitivity is consistent with the one provided by the manufacturer. In the high-frequency domain, the frequency response of the transducer exhibits two peaks, one of which is related to the resonance of the MEMS actuator. Future work will focus on the *in situ* calibration of wall-pressure sensors. The calibration procedure will let to a better identification of high-frequency instabilities in duct flows.

ACKNOWLEDGMENTS

The authors wish to express their most sincere thanks to Petr Yuldashev for the design and the realisation of the optical device.

This work has benefited from fruitful discussions with Christophe Bailly and Philippe Blanc-Benon. The authors are also grateful to Benoît Paoletti and Jean-Michel Perrin for their help in setting up the experiment.

This research has been funded by the French National Research Agency through the SIMMIC project (ANR-10-BLAN-0905). Financial support from the French National Research Agency through the SONOBL project (ANR-2011-BS09-035-02) is also acknowledged.

This work was performed within the framework of Labex CeLyA of Université de Lyon, operated by the (ANR-10-LABX-0060 / ANR-11-IDEX-0007).

REFERENCES

[1] J.F. Wilby, "Aircraft interior noise", *J. Sound Vib.* **190** (3), 2010.

[2] B. Arguillat, D. Ricot, C. Bailly & G. Robert, "Measured wavenumber: Frequency spectrum associated with acoustic and aerodynamic wall pressure fluctuations", *J. Acoust. Soc. Am.* **128** (4), 2010.

[3] E. Salze, C. Bailly, O. Marsden, E. Jondeau & D. Juvé, "An experimental characterisation of wall pressure wavevector-frequency spectra in the presence of pressure gradients", *20th AIAA/CEAS Aeroacoustics Conference*, n°2014-2909, 2014. (doi: 10.2514/6.2014-2909).

[4] N. Courtiade & X. Ottavy, "Experimental Study of Surge precursors in a high-speed multistage compressor", *J. of Turb.* **135**, 2013.

[5] G. Persico, P. Gaetani & A. Guardone, "Dynamic calibration of fast-response probes in low-pressure shock tubes", *Meas. Sci. Technol.* **16,** 2005.

[6] Kulite Pressure Transducer Handbook, Section 8.4, "Dynamic Calibration", 2006.

[7] P. Yuldashev, M. Averiyanov, V. Khokhlova O. Sapozhnikov, S. Ollivier & P. Blanc-Benon, "Measurement of shock N-waves using optical methods", *10ème Congrès Français d'Acoustique*, Lyon, France, n°193, 2010. (http://www.conforg.fr/cfa2010/cdrom/data/articles/000193.pdf).

[8] Zhou, Z. J., Rufer, L., Salze, E., Yuldashev, P., Ollivier, S. & Wong, M., "Bulk micro-machined wide-band aero-acoustic microphone and its application to acoustic ranging", *J. Micromech. Microeng.*, **23** (10), 2013.

[9] S. Ollivier, E. Salze, P. Yuldashev, C. Desjouy, M. Karzova, V. Khokhlova & P. Blanc-Benon, "Méthodes de calibration des microphones en hautes fréquences (10kHz - 1 MHz)", *12ème Congrès Français d'Acoustique*, Poitiers, France, n°362, 2014. (http://www.conforg.fr/cfa2014/cdrom/data/articles/000362.pdf)

[10] P. Yuldashev, S. Ollivier, M. Averiyanov, O. Sapozhnikov, V. Khokhlova & P. Blanc-Benon, "Nonlinear propagation of spark-generated N-waves in air: Modeling and measurements using acoustical and optical methods," *J. Acoust. Soc. Am.* **128**, 2010.

[11] E. Salze, P. Yuldashev, S. Ollivier, V. Khokhlova & P. Blanc-Benon, "Laboratory-scale experiment to study nonlinear N-wave distortion by thermal turbulence", *J. Acoust. Soc. Am.* **136** (2), 2014.

[12] G. Smeets, "Laser interference microphone for ultrasonics and nonlinear acoustics", *J. Acoust. Soc. Am.* **61**, 1977.